Supplementary 1.1 Sensitivity to number of tracers used

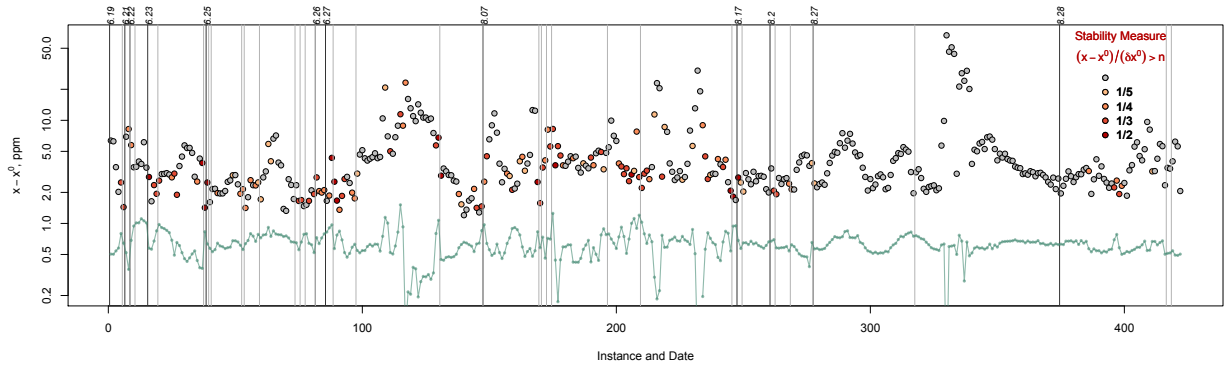

Figure S1: Estimate of variation in C_{burn} if x^0 is estimated by only three tracers (green dots:) and only five tracers (red dots). Green line repeats the pattern of $\widehat{\boldsymbol{x}}_{\boldsymbol{i}}^{\boldsymbol{0}} = C_{bkgd}$ shown with appropriate scale in Figure 8, for reference.

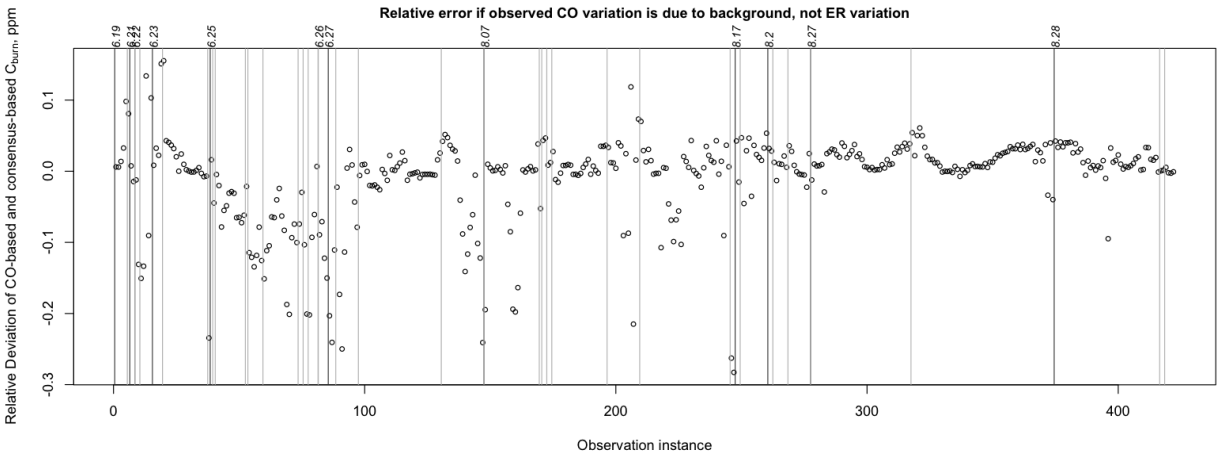

Figure S2 A heuristic measure of the stability of the situation.

The great variations in estimated $\hat{x}_i^0$ at a few points in Figure 9 can cause some concern (e.g. around sample numbered 8, 117, 130, 217m 231, 329, and 337) . Figure S2 suggests that sometimes these may be of concern, sometimes not. We constructed a measure of the temporal stability of the sampling situation by ratioing the changes of x0 to the amount of carbon burned, x-x0. The measure of change in ppm was

$$\text{Change Measure} = \left(\left|x_{i+1}^0 - x_i^0\right| + \left|x_i^0 - x_{i-1}^0\right|\right)/2$$

and to obtain a consistent measure of relative magnitude, an estimate of smoothed C_{burn} over the same span of i indices was also used,

$$\text{Magnitude Measure} = \left((x_{i-1} - x_{i-1}^0) + 2(x_i - x_i^0) + (x_{i+1} - x_{i+1}^0)\right)/4$$

This ratio of these gives our measure of the possible effect of relative change of actual C_{burn} during our the airborne measurements on the estimate of C_{burn} that the algorithm gives. Where the measurement crossed different plume boundaries (light gray lines in Figure 9), one-sided estimates consistent with these two values were calculated. We expect that use of absolute differences ratio may give a pessimistically high measure of potential influence; this was justified by a consideration of many different variations. The ratio Magnitude Measure / Change Measure can reach high values, where changes in x_i^0 can be 0.2, 0.25, 0.33, and 0.5 the amount of C_{burn}, as the colors of the points in Figure 8 show. Recall, however, that the neighboring x_i^0 estimates and C_{burn} estimates are derived independently, so the ratio does not correspond to traditional measures of high-frequency noise, only the stability and relation to identifiable processes on the ground. Figure S2 suggests that for some periods of high C_{burn}, variations of x_i^0 should matter little in calculations of C_{burn} or of the ER ratios derived from C_{burn}. In other periods, when C_{burn} is low, there can be reason for concern, even when sample-to-sample variability of x_i^0 is not especially high.

Supplementary 1.2 Examples of Enhancement Ratios

Methods used to prepare these graphs of EnRs for the two periods of observation, Figure S3 and Figure S4, are described in Sections.7 and 9.

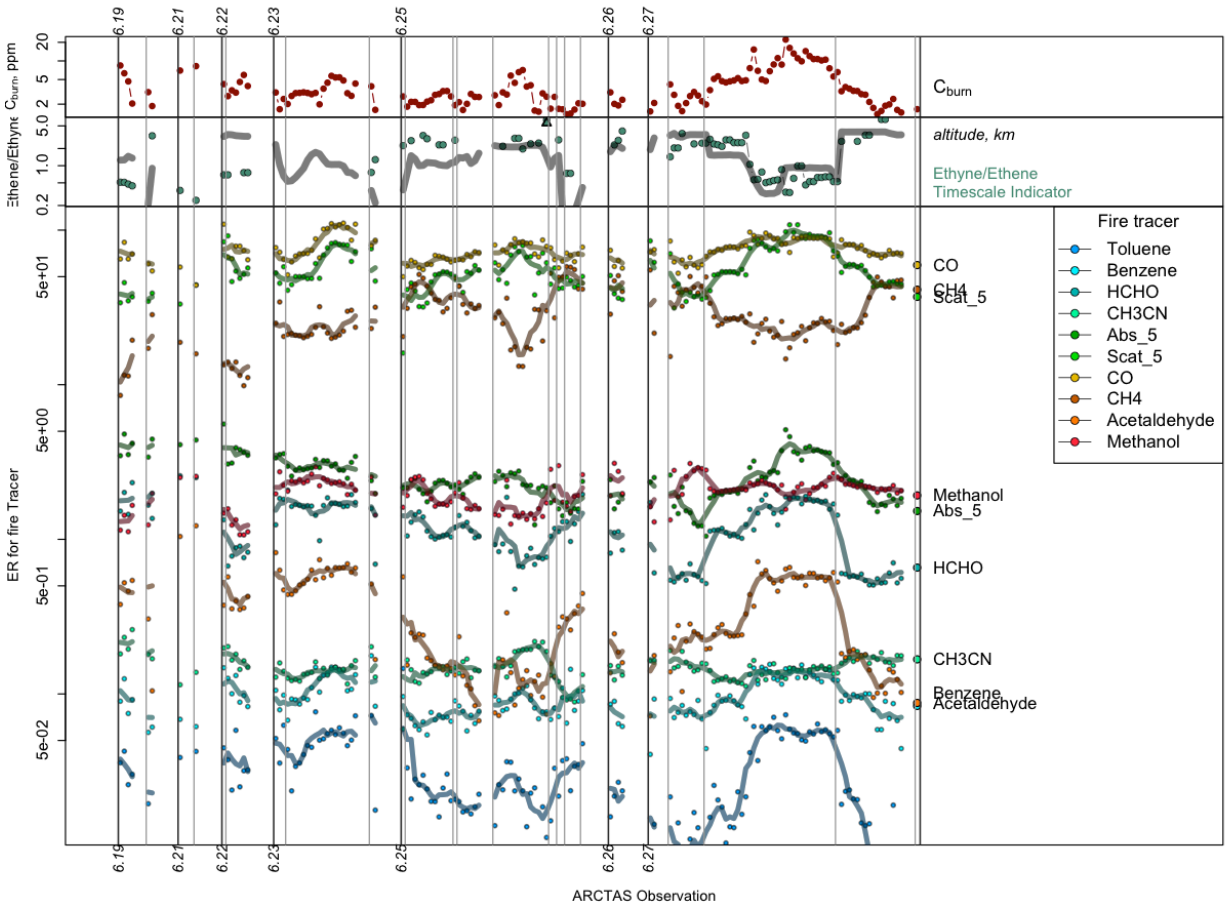

Figure S3. Estimates of C_{burn} , an ethyne/ethene photochemical transformation timescale, (Section 6.2), and enhancement ratios (EnRs) for each of the tracer compounds shown for all observations during the ARCTAS flights used in this analysis. Units for the EnRs are shown in Table 2. Some error measures for these EnRs, more detailed figures, and considerable interpretation appear in an analysis publication subsequent to this one (Chatfield and Andreae, 2019).

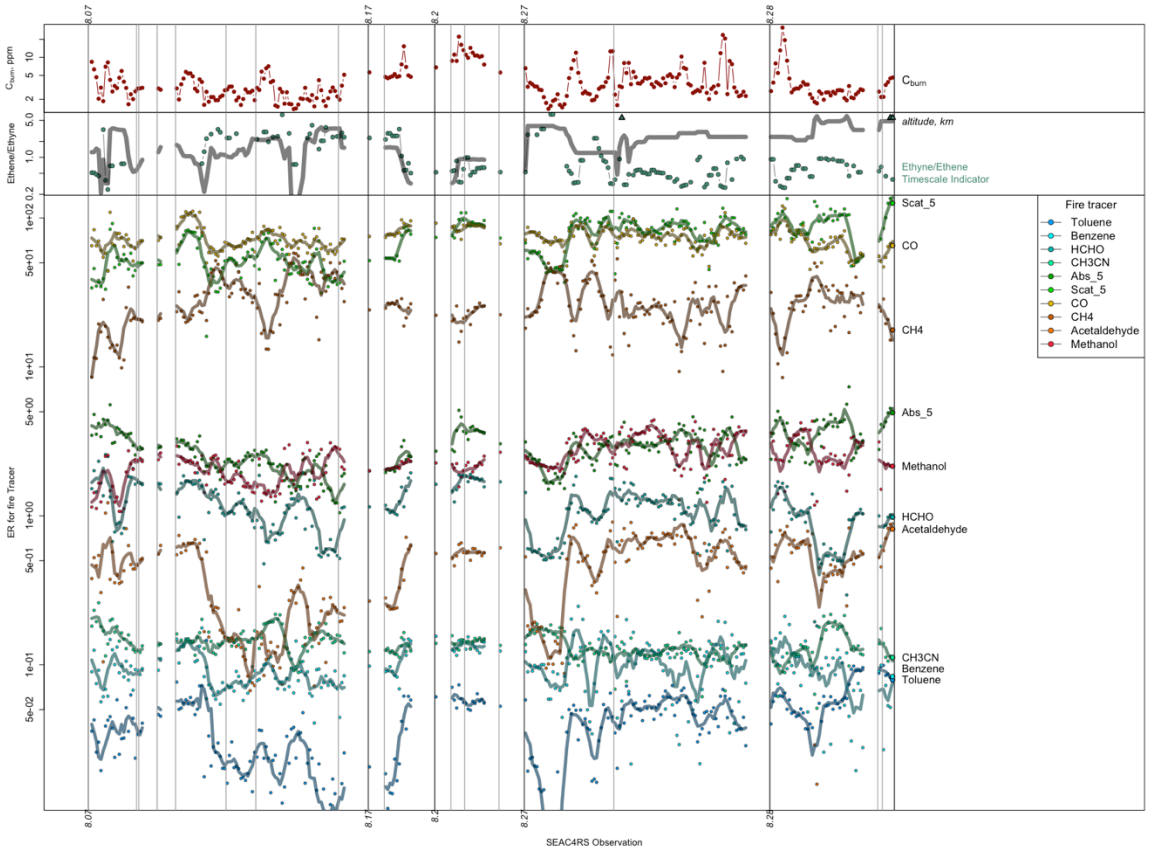

Figure S4. C_{burn} , an ethyne/ethene photochemical transformation timescale, (Section 6.2), and enhancement ratios (EnRs) for the SEAC4R observations. Units are given in Table 2.

Considerable further analysis will appear in Chatfield and Andreae (2019).